Chin. Ann. Math.
30B(6), 2009, 769–784
DOI: 10.1007/s11401-009-0101-x

Chinese Annals of Mathematics, Series B

Pattern Formations in Heat Convection Problems***

Takaaki NISHIDA* Yoshiaki TERAMOTO**

Abstract After Bénard's experiment in 1900, Rayleigh formulated heat convection problems by the Oberbeck-Boussinesq approximation in the horizontal strip domain in 1916. The pattern formations have been investigated by the bifurcation theory, weakly nonlinear theories and computational approaches. The boundary conditions for the velocity on the upper and lower boundaries are usually assumed as stress-free or no-slip. In the first part of this paper, some bifurcation pictures for the case of the stress-free on the upper boundary and the no-slip on the lower boundary are obtained. In the second part of this paper, the bifurcation pictures for the case of the stress-free on both boundaries by a computer assisted proof are verified. At last, Bénard-Marangoni heat convections for the case of the free surface of the upper boundary are considered.

Keywords Oberbeck-Boussinesq equation, Heat convection, Pattern formation, Computer assisted proof
2000 MR Subject Classification 65N15, 37M20, 35Q30

1 Introduction

We consider the Rayleigh-Bénard problem for the heat convection using the Oberbeck-Boussinesq equations for the velocity, pressure and temperature in the dimensionless form:

$$\begin{aligned}
&\frac{1}{\mathcal{P}_r}\Big(\frac{\partial \vec{u}}{\partial t}+\vec{u}\cdot\nabla\vec{u}\Big)+\nabla p=\Delta\vec{u}-\rho(T)\nabla z,\\
&\nabla\cdot\vec{u}=0,\\
&\frac{\partial T}{\partial t}+\vec{u}\cdot\nabla T=\Delta T,
\end{aligned}$$

in the horizontal domain $\{-\infty<x,y<+\infty,\ 0\le z\le 1\}$, where $\mathcal{P}_r$ is the Prandtl number, $\mathcal{R}_a$ is the Rayleigh number, and $\rho(T)=\mathrm{G}-\mathcal{R}_aT$ is assumed for the density of the fluid to take into account of the buoyancy effect.

When the temperature $T=1$ is given on the lower boundary and $T=0$ on the upper boundary, the equilibrium state is given by the purely heat conduction solution, which exists for all parameter values:

$$\begin{aligned}
&\vec{u}=0,\quad T=1-z,\quad \rho=\mathrm{G}-\mathcal{R}_a(1-z),\\
&p=\mathrm{G}(1-z)-\mathcal{R}_a\Big(\frac{1}{2}-z+\frac{z^2}{2}\Big)+p_{\mathrm{atmosphere}}.
\end{aligned}$$

Manuscript received March 31, 2009. Published online September 25, 2009.
*Department of Mathematics, Waseda University, Tokyo 169-8555, Japan. E-mail: tkknish@waseda.jp
**Department of Mathematics and Physics, Setsunan University, Neyagawa 572-8508, Japan. E-mail: teramoto@mpg.setsunan.ac.jp
***Project supported by JSPS KAKENHI (No. 20540141).

Thus we want to consider the stability of the heat conduction state by the system for the perturbations in the dimensionless form:

$$\begin{aligned}
&\frac{1}{\mathcal{P}_r}\Big(\frac{\partial \vec{u}}{\partial t} + \vec{u}\cdot\nabla\vec{u}\Big) + \nabla p = \Delta\vec{u} + \mathcal{R}_a\theta\nabla z,\\
&\nabla\cdot\vec{u} = 0,\\
&\frac{\partial\theta}{\partial t} + \vec{u}\cdot\nabla\theta = \Delta\theta + w.
\end{aligned}$$

These equations have the equilibrium solution $\vec{u} = \vec{0}$, $\theta = 0$ for any Rayleigh and any Prandtl numbers, which represents the purely heat conducting state. We consider the problem in the domain $\{-\infty < x, y < +\infty,\ 0 \le z \le 1\}$ with the periodic boundary conditions with respect to x and y,

$$0 \le x \le \frac{2\pi}{a}, \quad 0 \le y \le \frac{2\pi}{b}.$$

The boundary conditions for the velocity are stress free on the both boundaries:

$$\frac{\partial u}{\partial z} = \frac{\partial v}{\partial z} = w = \theta = 0, \quad \text{on } z = 0, 1,$$

or they are stress free on the upper surface and fixed on the bottom:

$$\begin{aligned}
&\frac{\partial u}{\partial z} = \frac{\partial v}{\partial z} = w = \theta = 0, \quad \text{on } z = 1,\\
&u = v = w = \theta = 0, \qquad\quad \text{on } z = 0.
\end{aligned}$$

At last, we consider a Bénard-Marangoni problem, i.e., the free boundary condition for the velocity on the upper surface and the fixed BC on the bottom:

$$\begin{aligned}
&\frac{\partial\eta}{\partial t} = u_3 - \vec{u}_h\cdot\nabla_h\eta|_{z=\eta(t,x,y)},\\
&((p - p_{\text{air}})I - (\nabla\vec{u} + \nabla^t\vec{u}))\cdot\vec{n} = \sigma 2H\vec{n} + (\vec{\tau}\cdot\nabla)\sigma\vec{\tau},\\
&\vec{n}\cdot\nabla T + \mathcal{B}_i T = -1, \quad \text{on } z = \eta(t,x,y).
\end{aligned}$$

Here the fluid domain is given by $\{-\infty < x, y < +\infty,\ 0 \le z \le \eta(t,x,y)\}$, where $z = \eta(t,x,y)$ is its free surface, $\mathcal{M}_a$ is the Marangoni number, and σ is the surface tension,

$$\sigma \equiv \mathcal{C}_a - \mathcal{M}_a T, \quad 2H \equiv \nabla_h\Big(\frac{\nabla_h\eta}{\sqrt{1 + |\nabla_h\eta|^2}}\Big).$$

2 Stress Free Upper Boundary and Fixed Bottom Boundary

We want to apply the usual bifurcation theory to the system in the case of the stress free upper boundary and the fixed bottom boundary. Then we have to consider the linearized system to see the critical Rayleigh number from which stationary bifurcations occur:

$$\begin{aligned}
&\frac{\partial\vec{u}}{\partial t} + \mathcal{P}_r\nabla p = \mathcal{P}_r\Delta\vec{u} + \mathcal{P}_r\mathcal{R}_a\theta\nabla z,\\
&\nabla\cdot\vec{u} = 0,\\
&\frac{\partial\theta}{\partial t} = \Delta\theta + w,
\end{aligned}$$

where the domain and the boundary conditions are the following:

$$
\begin{aligned}
&0 \le x \le \frac{2\pi}{a}, \quad 0 \le y \le \frac{2\pi}{b}, \quad 0 \le z \le 1,\\
&\frac{\partial u}{\partial z} = \frac{\partial v}{\partial z} = w = \theta = 0, \quad \text{on } z = 1,\\
&u = v = w = \theta = 0, \quad \text{on } z = 0.
\end{aligned}
$$

Now we consider the stability of the linearized systems under the periodic boundary conditions in the horizontal direction and also assume usual even- or odd-ness of functions for all perturbations as follows:

$$
\begin{aligned}
u(x,y,z) &= -u(-x,y,z) = u(x,-y,z),\\
v(x,y,z) &= v(-x,y,z) = -v(x,-y,z),\\
w(x,y,z) &= w(-x,y,z) = w(x,-y,z),\\
\theta(x,y,z) &= \theta(-x,y,z) = \theta(x,-y,z),\\
p(x,y,z) &= p(-x,y,z) = p(x,-y,z).
\end{aligned}
$$

The function space for the solutions u, v, w, θ is the Sobolev space $H^2_{a,b}$, which consists of square integrable functions $L^2_{a,b}$ up to the second derivatives with the above periodicity. Then the system is self-adjoint in this case, and the first component of velocity and the temperature may have the expansions

$$
\begin{aligned}
u(t,x,y,z) &= \sum_{l,m} u_{lm}(t,z)\sin(alx)\cos(bmy),\\
\theta(t,x,y,z) &= \sum_{l,m} \theta_{lm}(t,z)\cos(alx)\cos(bmy).
\end{aligned}
$$

The other unknowns have similar expressions. Thus the system for the eigenvalue problem can be obtained as the system of ordinary differential equations with respect to z for each fixed horizontal mode (l,m):

$$
\begin{aligned}
&\lambda u_{l,m} - \mathcal{P}_r alp_{l,m} = \mathcal{P}_r\Big\{\frac{\mathrm{d}^2}{\mathrm{d}z^2} - (a^2l^2 + b^2m^2)\Big\}u_{l,m},\\
&\lambda v_{l,m} - \mathcal{P}_r bmp_{l,m} = \mathcal{P}_r\Big\{\frac{\mathrm{d}^2}{\mathrm{d}z^2} - (a^2l^2 + b^2m^2)\Big\}v_{l,m},\\
&\lambda w_{l,m} + \mathcal{P}_r\frac{\mathrm{d}}{\mathrm{d}z}p_{l,m} = \mathcal{P}_r\Big\{\frac{\mathrm{d}^2}{\mathrm{d}z^2} - (a^2l^2 + b^2m^2)\Big\}w_{l,m} + \mathcal{P}_r\mathcal{R}_a\theta_{l,m},\\
&\lambda\theta_{l,m} = \Big\{\frac{\mathrm{d}^2}{\mathrm{d}z^2} - (a^2l^2 + b^2m^2)\Big\}\theta_{l,m} + w_{l,m},\\
&alu_{lm} + bmv_{lm} + \frac{\mathrm{d}}{\mathrm{d}z}w_{lm} = 0, \quad 0 < z < 1,\\
&\frac{\mathrm{d}u}{\mathrm{d}z} = \frac{\mathrm{d}v}{\mathrm{d}z} = w = \theta = 0, \quad \text{on } z = 1,\\
&u = v = w = \theta = 0, \quad \text{on } z = 0.
\end{aligned}
$$

In order to obtain the eigenvalues and eigen-vectors, especially for those of $\lambda = 0$, all of which are real, we need numerical computations. For each (l,m)-mode to obtain the critical Rayleigh

number which corresponds to $\lambda = 0$, we may use the Chebyshev polynomial expansion in $0 \le z \le 1$ for the system of ordinary differential equations.

$$w_{l,m}(\lambda, z) = \sum_n w_{l,m,n}(\lambda) T_n(2z+1).$$

Then, by the numerical computations, we can obtain the following value and critical Rayleigh number, at which the largest eigenvalue becomes zero,

$$a = 0.42685\cdots > \frac{1}{2\sqrt{2}} = 0.35355\cdots,$$
$$\mathcal{R}_c = 1100.6\cdots > 6.75 \times \pi^4 = 657.51\cdots.$$

The values of the right-hand side of the inequalities correspond to those for the stress free boundary condition on both boundaries, which can be obtained in the explicit forms.

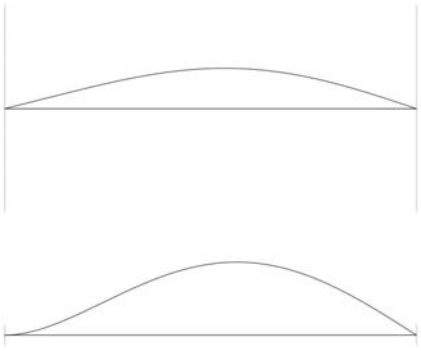

Figure 1 Eigenfunctions of θ and w

We see that these eigen-functions in Figure 1 satisfy the boundary conditions:

$$w = \frac{\mathrm{d}w}{\mathrm{d}z} = \theta = 0, \quad \text{on } z = 0, \quad w = \frac{\mathrm{d}^2 w}{\mathrm{d}z^2} = \theta = 0, \quad \text{on } z = 1.$$

These eigenvalue and eigen-functions are verified in a way similar to that in [9]. We see from the above linearized analysis that

(i) if $\mathcal{R}_a < \mathcal{R}_c$, then the heat conduction state is linearly stable;

(ii) if $\mathcal{R}_a > \mathcal{R}_c$, then the heat conduction state is linearly unstable.

Furthermore, in 1965, Joseph proved by the energy method and variational formulation that if $\mathcal{R}_a < \mathcal{R}_c$, then the heat conduction state is globally nonlinearly stable.

In fact, let

$$w = \vec{u}_3, \quad \widetilde{\theta} = \sqrt{\mathcal{R}_a}\,\theta, \quad \nabla \cdot \vec{u} = 0.$$

We compute the usual energy in the form:

$$\frac{\mathrm{d}}{\mathrm{d}t}\frac{1}{2}\int \Big(\frac{|\vec{u}|^2}{\mathcal{P}_r} + \widetilde{\theta}^{\,2}\Big)\mathrm{d}x\mathrm{d}y\mathrm{d}z + \int (|\nabla \vec{u}|^2 + |\nabla \widetilde{\theta}\,|^2)\mathrm{d}x\mathrm{d}y\mathrm{d}z$$
$$= 2\sqrt{\mathcal{R}_a}\int (w\widetilde{\theta}\,)\mathrm{d}x\mathrm{d}y\mathrm{d}z \le \int (\mathcal{R}_a|\nabla^{-1}w|^2 + |\nabla\widetilde{\theta}\,|^2)\mathrm{d}x\mathrm{d}y\mathrm{d}z.$$

Thus the critical Rayleigh number $\mathcal{R}_c$ is determined by

$$\mathcal{R}_c = \sup 2 \int w\widetilde{\theta}\,\mathrm{d}x\mathrm{d}y\mathrm{d}z, \quad \text{under } \int (|\nabla \vec{u}|^2 + |\nabla\widetilde{\theta}|^2)\mathrm{d}x\mathrm{d}y\mathrm{d}z = 1,\ \nabla\cdot\vec{u} = 0.$$

The Euler-Lagrange equation is the zero-eigenvalue problem of the linearized equation.

The first (biggest) eigenvalue crossing the origin $\lambda = 0$ with a nonzero velocity determines the critical Rayleigh number ($\mathcal{R}_c$) for the stationary bifurcation.

Theorem 2.1 (Simple Bifurcation Theorem) (see [4]) *Let U and V be Banach spaces, and $\mathcal{F}(u,\mu)$ be a twice continuously differentiable map from a neighbourhood of the origin of $U \times R$ into V and $\mathcal{F}(0,\mu) = 0$ for any μ.*

(i) *Assume that the null space $\mathcal{N}(D_u\mathcal{F}(0,0))$ is one-dimensional and spanned by u_0.*

(ii) *The co-dimension of the range $\mathcal{R}(D_u\mathcal{F}(0,0))$ is also one.*

(iii) *Assume $D_{u,\mu}\mathcal{F}(0,0)u_0 \notin \mathcal{R}(D_u\mathcal{F}(0,0))$.*

Then the solutions for the equation $\mathcal{F}(u,\mu) = 0$ in a neighbourhood of $(0,0)$ are composed of $\{(0,\mu)\} \cup \{(su_0 + s\phi(s), \mu(s))\}$. Here $\phi(s)$ and $\mu(s)$ are continuously differentiable in $-s_0 < s < s_0$, $\phi(s) \in \mathcal{R}(D_u\mathcal{F}(0,0))$ and $\phi(0) = 0$, $\mu(0) = 0$.

3 Solution of the Roll-Type, Rectangle-Type and Hexagon-Type

To see pattern formations after the bifurcation clearly, let us take $a = 0.42685\cdots$ and $b = \sqrt{3}\,a$. In this case, $(al)^2 + (bm)^2$ is the same for $(l,m) = (2,0)$ and $(l,m) = (1,1)$, and so the eigenvalue $\lambda = 0$ has a two-dimensional eigenspace at $\mathcal{R}_c = 1100.6\cdots$.

The roll-type solution corresponds to the mode $(l,m) = (2,0)$, and the eigenfunction for the temperature is

$$\theta = \theta_{20}(z)\cos(2ax).$$

The rectangle-type solution corresponds to the mode $(l,m) = (1,1)$, and its eigenfunction for the temperature has the expression

$$\theta = \theta_{11}(z)\cos(ax)\cos(\sqrt{3}\,ay).$$

The hexagon-type solution is a linear combination of them, and the eigenfunction for the temperature has the expression

$$\theta = \theta_{\mathrm{hex}}(z)\{2\cos(ax)\cos(\sqrt{3}\,ay) + \cos(2ax)\}.$$

The eigenspace has two dimensions, and we have to restrict the function space $H^2_{a,\sqrt{3}\,a}$ for the solution to the subspace in order to apply the simple bifurcation theory.

First, we restrict the space to the subspace of roll-type solution $H^2_{\mathrm{roll}} \subset\subset H^2_{a,\sqrt{3}\,a}$. In this subspace, the zero eigenvalue becomes simple because the temperature for example has the expression in this subspace:

$$\theta = \sum_{n=0}^{\infty}\sum_{l=\mathrm{even}}^{\infty} \theta_{l,0,n}\cos(alx)T_n(2z+1).$$

Thus we have the bifurcation of roll-type solutions in the direction of $\mathcal{R}_a > \mathcal{R}_c = 1100.6\cdots$.

The hexagonal solution has the rotational invariance of $\frac{2\pi}{3}$ in the x-y plane and is obtained in the subspace $H^2_{\rm hexa}$:

$$\theta = \sum_{l,m,n}^{\infty} \theta_{l,m,n}\Big\{ \cos(alx)\cos(\sqrt{3}\,amy) + \cos\Big(a\Big(\frac{l-3m}{2}\Big)x\Big)\cos\Big(\sqrt{3}\,a\Big(\frac{l+m}{2}\Big)y\Big) + \cos\Big(a\Big(\frac{l+3m}{2}\Big)x\Big)\cos\Big(\sqrt{3}\,a\Big(\frac{l-m}{2}\Big)y\Big)\Big\}T_n(2z+1).$$

Although there is another eigenfunction which corresponds to a rectangle type solution (see mode $(1,1)$), the bifurcation from this eigenfunction is not clear from the simple bifurcation theorem. It will be seen later in the bifurcation picture obtained by a numerical computation for the mixed type solution (see Figures 5 and 6).

These bifurcated solutions come out of the zero solution at the same critical Rayleigh number $\mathcal{R}_c = 1100.6\cdots$ in the direction of $\mathcal{R}_a > \mathcal{R}_c$, and they belong to their own subspaces, i.e., they are independent in the function space. They are stable in their subspaces for the time evolution of the linearized system. But the stability in the original function space $H^2_{a,\sqrt{3}\,a}$ is not known by the simple bifurcation theorem. The stability of these solutions in the original function space $H^2_{a,\sqrt{3}\,a}$ can be determined by the center manifold theory in a neighborhood of the bifurcation point (see [3, 6, 7]).

Now the main problem is to obtain global bifurcation diagrams and to see the global structure of the solution space. At least, we want to know how to extend the bifurcation curves, how to analyze the stability of the solution on the extended branches and how to investigate other bifurcations on them, i.e., the secondary bifurcations and so on.

4 Global Bifurcation Curves

To extend the bifurcated stationary solution curves, we need to do numerical computations for the nonlinear system:

$$\begin{aligned} &\frac{1}{\mathcal{P}_r}\vec{u}\cdot\nabla\vec{u} + \nabla p = \Delta\vec{u} + \mathcal{R}_a\theta\nabla z,\\ &\nabla\cdot\vec{u} = 0,\\ &\vec{u}\cdot\nabla\theta = \Delta\theta + w. \end{aligned}$$

Thus we may use the Chebyshev polynomial expansion for the solutions in $0 \le z \le 1$.

$$w(t,x,y,z) = \sum_{l,m,n} w_{lmn}\cos(alx)\cos(bmy)T_n(2z+1).$$

Then $\{u_{l,m,n}, v_{l,m,n}, w_{l,m,n}, \theta_{l,m,n}, p_{l,m,n}\}$ are unknowns of infinite number and should satisfy the second order algebraic equations of infinite number.

We approximate the system by Galerkin method for unknowns of finite number

$$\{u_{l,m,n}, v_{l,m,n}, w_{l,m,n}, \theta_{l,m,n}, p_{l,m,n},\ l+m \le M,\ n \le N\}.$$

For each horizontal mode (l,m), we have $5\times(N+1)$ unknowns for u,v,w,θ,p, which should satisfy $4\times 2 = 8$ boundary conditions for u,v,w,θ, $3\times(N-1)$ equations for u,v,θ, $2\times N$ equations for w, and div-free condition for our Galerkin-τ approximation.

Let U be the unknowns of finite number and write the system in the form

$$F(U;\mathcal{R}_a,\mathcal{P}_r)=0.$$

We solve these equations of finite number by Newton method for fixed $\mathcal{R}_a$ and $\mathcal{P}_r$:

$$U_{k+1}=U_k-DF(U_k)^{-1}F(U_k),\quad k=0,1,2,\cdots,$$

where $DF(U_k)$ is the Fréchet derivative at U_k, and we choose U_0 appropriately.

We do numerical computations by Newton method for the solution of roll-, hexagon- and mixed-type.

4.1 Roll-type solution

Figure 2 is the cross sections of two solutions of roll type for $\mathcal{R}_a=2\times\mathcal{R}_c$ and $\mathcal{R}_a=10\times\mathcal{R}_c$. The fluid is going up around the center of the solutions.

Figure 3 shows the bifurcation curve of roll type solution, where x-axis is for the normalized Rayleigh number, and y-axis is for the coefficient $u_{2,0,1}$ of the solution.

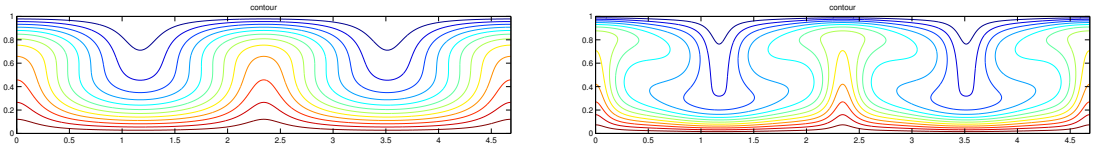

Figure 2 The isothermal line (the red-lined fluid is warmer than the blue-lined one) on the cross section $y=$ constant

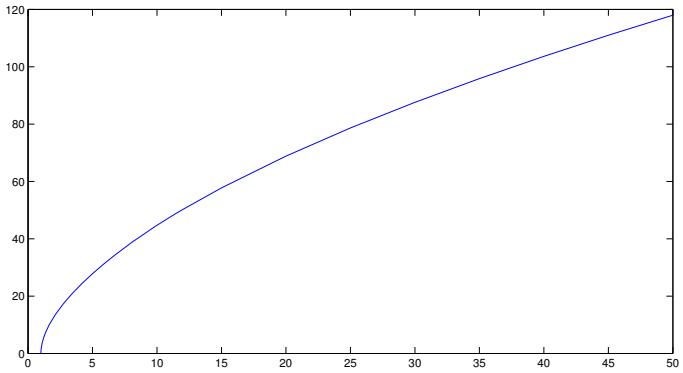

Figure 3 The solution curves of roll type for $1.0\le r=\frac{\mathcal{R}_a}{\mathcal{R}_c}\le 50.0$

4.2 Hexagonal solutions

Figure 4 is two hexagonal solutions for $\mathcal{R}_a=1.5\times\mathcal{R}_c$. The fluid is sinking around the center of the hexagon on the left one and is going up on the right one. The figure shows the isothermal line on the one-period domain in $x-y$ plane of $z=\frac{1}{2}$.

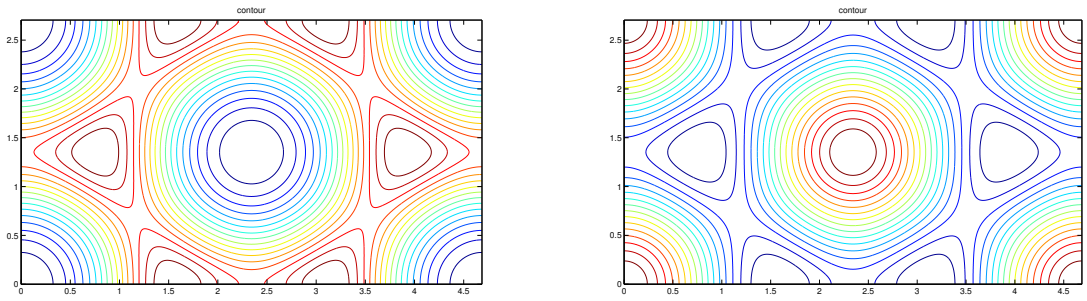

Figure 4 The isothermal line on the middle horizontal plane $z = \frac{1}{2}$ (hexagonal type)

4.3 Mixed type solution

We also have solutions of mixed type of rectangle and hexagon: the left one in Figure 5 is a solution of mixed type for $\mathcal{R}_a = 1.1 \times \mathcal{R}_c$ and the right one is for $\mathcal{R}_a = 1.6 \times \mathcal{R}_c$.

The bifurcation curve of these mixed type solutions begins from the first bifurcation point $\mathcal{R}_a = \mathcal{R}_c$, where it corresponds to the eigenfunction of rectangle type. The bifurcation curves for the hexagonal solution and the solution of mixed type, of which the fluid is sinking around the center, are given in Figure 6. The hexagonal solution has larger values of $u_{2,0,1}$ than those of mixed type near the bifurcation point $r = 1$. The x-axis is for the normalized Rayleigh number and y-axis is for the coefficient $u_{2,0,1}$.

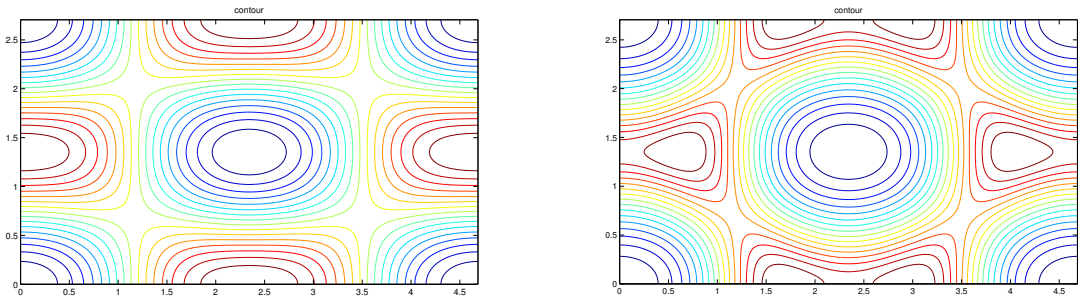

Figure 5 The isothermal line on the middle horizontal plane $z = \frac{1}{2}$ (mixed type)

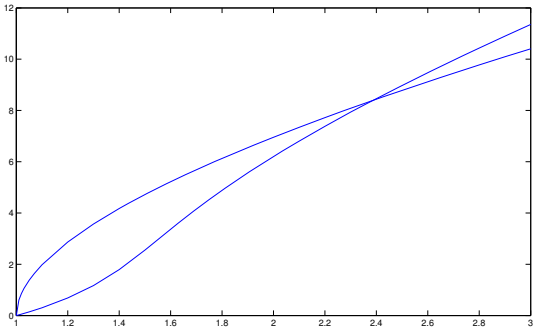

Figure 6 The solution curves of hexagonal type and of mixed type for $1.0 \leq r = \frac{\mathcal{R}_a}{\mathcal{R}_c} \leq 3.0$, whose cooler fluids (blue-lined) are sinking around the center.

There are other solutions of mixed type which correspond to the hexagonal solution of which the fluid is going up around the center. The left one in Figure 7 is a solution of mixed type for $\mathcal{R}_a = 1.63 \times \mathcal{R}_c$ and the right one is for $\mathcal{R}_a = 1.80 \times \mathcal{R}_c$.

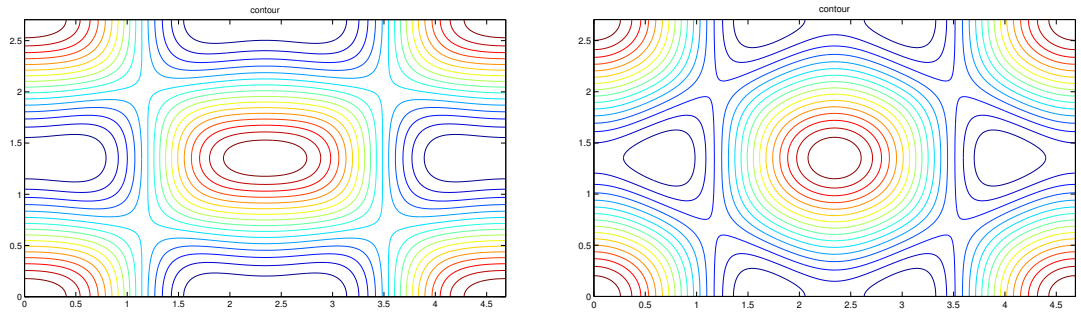

Figure 7 The isothermal line on the middle horizontal plane $z = \frac{1}{2}$ (other mixed type)

The solution curve of this mixed type does not come from the first bifurcation point $(r, u_{2,0,1}) = (1, 0)$ and approaches to that of hexagonal solution, of which the fluid is going up around the center. In fact, we have the bifurcation curves which cross near $\mathcal{R}_a = 2.02 \times \mathcal{R}_c$ in Figure 8. The x-axis is for the normalized Rayleigh number, and the y-axis is for the coefficient $u_{2,0,1}$ as before.

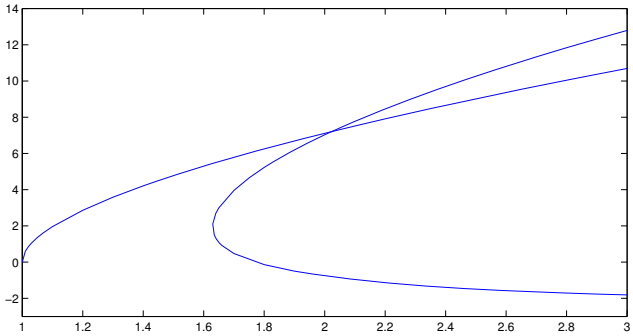

Figure 8 The solution curves of hexagonal solution and of mixed type for $1.0 \leq r = \frac{\mathcal{R}_a}{\mathcal{R}_c} \leq 3.0$, whose warmer fluids (red-lined) are going up around the center.

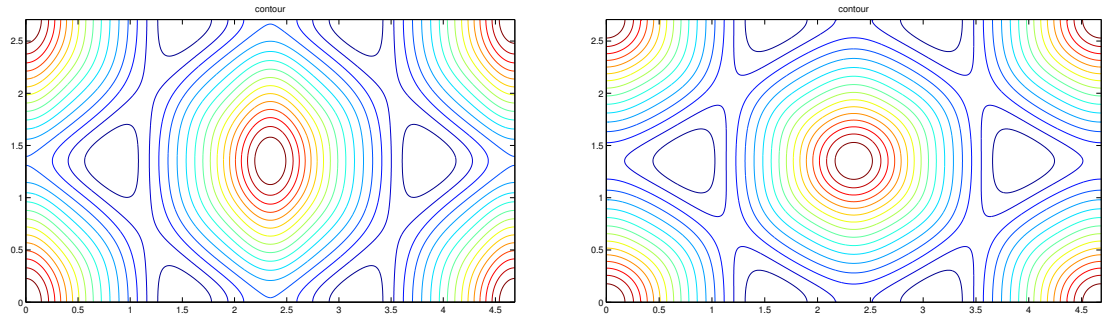

Figure 9 The isothermal line on the middle horizontal plane $z = \frac{1}{2}$

Figure 9 shows the mixed type solution and hexagonal solution for $\mathcal{R}_a = 3 \times \mathcal{R}_c$ after the intersection of the solution curves. Although the hexagonal solution keeps equilateral, the hexagon of mixed type solution is elongated in the y-direction after the intersection.

5 Computer Assisted Proof for the Solution in the Large

We consider a constructive approximation to the solution in the large for the system of semilinear partial differential equations. We have a theorem which guarantees the existence of a genuine solution in a small neighbourhood of a "good" approximate solution. These ideas have been used by Urabe in 1960's for the system of ordinary differential equations. It is a simplified Newton method by the Schauder's fixed point theorem in the following setting.

Let $U \subset V \subset W$ be Banach spaces, in which the embedding $U \subset V$ is compact. Consider the semilinear equation

$$\mathcal{F}(u) \equiv Au + B(u,u) = 0,$$

where $A : U \longmapsto W$ is a linear operator, and $B : V \times V \longmapsto W$ is a bilinear operator such that

$$\|B(u,v)\|_W \le K_2\|u\|_V\|v\|_V, \quad \|B(u,v)\|_V \le K_2\|u\|_U\|v\|_U.$$

The N-dimensional projection $P_N : u \in W \longmapsto W_N$ satisfies the following for any $N > 0$ and commutes with A:

$$\forall\, v \in V, \quad v_N = P_N v, \quad \|v_N - v\|_W \le \frac{1}{N}\|v\|_V,$$
$$\forall\, u \in U, \quad u_N = P_N u, \quad \|u_N - u\|_V \le \frac{1}{N}\|u\|_U.$$

Theorem 5.1 *Let $\overline{u} \in U_N$ be a good approximate solution in the sense that*

$$A\overline{u} + P_N B(\overline{u},\overline{u}) = R_N, \quad \|R_N\|_W < \epsilon \ll 1,$$

and that for the linearized equation at this approximate solution:

$$L(\overline{u})v \equiv Av + B(\overline{u},v) + B(v,\overline{u}) = f.$$

Then there exist its inverse and a constant $K_1 < \infty$ such that

$$\|L(\overline{u})^{-1}f\|_U \le K_1\|f\|_W.$$

If $\epsilon_1 = \|B(\overline{u},\overline{u}) - P_N B(\overline{u},\overline{u})\|_W \ll 1$, and if we can find an α such that

$$K_1(\epsilon + \epsilon_1 + K_2\alpha^2) < \alpha,$$

then there exists a genuine solution $u \in U$ in $\mathcal{W} = \{\|u - \overline{u}\|_V < \alpha\}$.

Idea of the Proof Let us look for the solution in the form $u = \overline{u} + v$. Let us define, for any $v \in \mathcal{W}$,

$$\mathcal{F}(v) \equiv -L(\overline{u})^{-1}\{(A\overline{u} + P_N B(\overline{u},\overline{u})) + (B(\overline{u},\overline{u}) - P_N B(\overline{u},\overline{u})) + B(v,v)\}.$$

Then, by the assumption for $\mathcal{W}$ and α, we have $\mathcal{F}(\mathcal{W}) \subset \mathcal{W}$ and the Schauder fixed point theorem gives the theorem.

5.1 Roll-type solutions in the large

In order to obtain the roll-type solution for large Rayleigh number, we use the stream function instead of the velocity because of two-dimension:

$$\frac{\partial}{\partial t}\Delta\psi = \mathcal{P}_r\mathcal{R}a\Delta^2\psi + \mathcal{R}a\frac{\partial\theta}{\partial x} + \frac{\partial\psi}{\partial z}\frac{\partial\Delta\psi}{\partial x} - \frac{\partial\psi}{\partial x}\frac{\partial\Delta\psi}{\partial z},$$
$$\frac{\partial\theta}{\partial t} = \Delta\theta + \frac{\partial\psi}{\partial x} + \frac{\partial\psi}{\partial z}\frac{\partial\theta}{\partial x} - \frac{\partial\psi}{\partial x}\frac{\partial\theta}{\partial z}.$$

When the both upper and lower boundary conditions for the velocity are stress free, the solution has the expansion

$$\psi(t,x,z) = \sum_{l,n}\psi_{ln}(t)\sin(alx)\sin(n\pi z), \quad \theta(t,x,z) = \sum_{l,n}\theta_{ln}(t)\cos(alx)\sin(n\pi z).$$

The function space for the solution is $H^4 \otimes H^2$ with this horizontal periodicity.

The bifurcation curves of stationary roll-type solutions can be obtained by Galerkin approximation of the system for unknowns with finite number $l + n \le N$ and by Newton method as before.

Figure 10 shows the bifurcation curve of roll-type solutions of mode $(l, n) = (2, 1)$. Here $a = \frac{1}{2\sqrt{2}}$, and the x-axis is for the Rayleigh number and y-axis is for $\psi_{2,1}$.

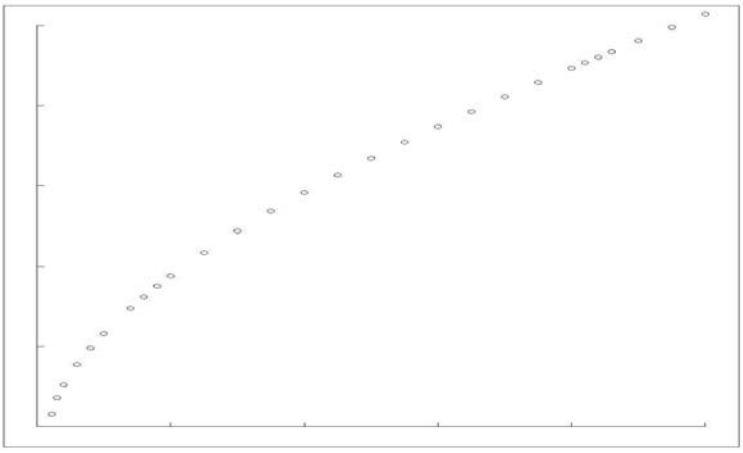

Figure 10 Bifurcation curve of roll-type solution of mode $(2, 1)$ for $0 \le \mathcal{R}_a \le 50 \times \mathcal{R}_c$

This roll-type solution is stable for $\mathcal{R}_a < 41 \times \mathcal{R}_c$, but the eigenvalue of the linearized system around these roll-type solution crosses the imaginary axis at about Rayleigh number $\mathcal{R}_a \simeq 42 \times \mathcal{R}_c$. Then it becomes unstable and there occurs the Hopf bifurcation. The shape of the roll-type solution almost does not change before and after the stability change as shown in Figure 11.

In order to prove the existence of these roll-type solutions far from the first bifurcation point $\mathcal{R}_a = \mathcal{R}_c$, we transform the problem to a fixed point formulation in the function space $H^3 \otimes H^1$

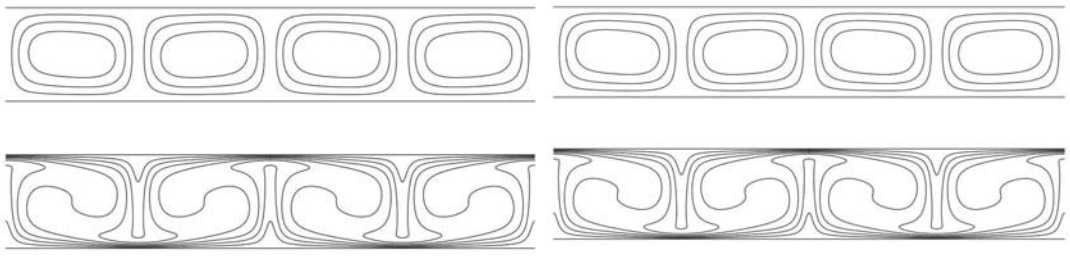

Figure 11 Roll-type solution of mode $(2,1)$ for $\mathcal{R}_a = 40 \times \mathcal{R}_c$ and $\mathcal{R}_a = 43 \times \mathcal{R}_c$

with the help of the inverse operator of Δ^2 and Δ with the boundary conditions

$$\psi = \frac{1}{\mathcal{P}_r \mathcal{R}_a}\Big\{\Delta^{-2}\Big(\mathcal{R}_a \frac{\partial \theta}{\partial x} + \frac{\partial \psi}{\partial z}\frac{\partial \Delta\psi}{\partial x} - \frac{\partial \psi}{\partial x}\frac{\partial \Delta\psi}{\partial z}\Big)\Big\},$$
$$\theta = \Delta^{-1}\Big(\frac{\partial \psi}{\partial x} + \frac{\partial \psi}{\partial z}\frac{\partial \theta}{\partial x} - \frac{\partial \psi}{\partial x}\frac{\partial \theta}{\partial z}\Big).$$

The nonlinear operators on the right-hand side are compact in the space $H^3 \otimes H^1$. We write them as $\mathcal{F}_0$. We look for the solution

$$\mathcal{F}_0(\psi, \theta) = (\psi, \theta).$$

The solution is sought in the form

$$(\psi, \theta) = (\overline{\psi}_N, \overline{\theta}_N) + (w^{(1)}, w^{(2)}),$$

where $(\overline{\psi}_N, \overline{\theta}_N)$ is a numerically computed good solution. Then the equation can be written for $w = (w^{(1)}, w^{(2)})$ as

$$\mathcal{F}(w) = w.$$

Therefore, for fixed $\mathcal{R}_a$ and $\mathcal{P}_r$, if we find a bounded closed convex set $\mathcal{W}$ in the function space $H^3 \otimes H^1$ and prove

$$\mathcal{F}(\mathcal{W}) \subset \mathcal{W},$$

then there exists a fixed point in $\mathcal{W}$ by Schauder theorem, which proves the existence of the roll type solution. This set $\mathcal{W}$ is constructed as a small neighborhood of the origin. The inclusion $\mathcal{F}(\mathcal{W}) \subset \mathcal{W}$ is verified by numerical computations as a computer assisted proof. In fact, we decompose the set by the orthogonal projection P_N,

$$\mathcal{W} = \mathcal{W}_N \oplus \mathcal{W}_N^{\perp},$$

where $\mathcal{W}_N = P_N \mathcal{W}$ is a finite dimensional small neighborhood of the origin, and $\mathcal{W}_N^{\perp}$ is a small neighborhood of zero in the orthogonal subspace with infinite dimension. The finite dimensional part is estimated by a simplified Newton method, and the infinite dimensional part is estimated by the norm. Both estimates need the interval arithmetic by computer for the error estimate.

At present, the case for $\mathcal{R}_c < \mathcal{R}_a \le 10 \times \mathcal{R}_c$ can be verified by our computer assisted proof in the case of two-dimensional problems (see [23]).

Three dimensional problems, namely for the hexagonal solution and rectangular solution, can be verified for small normalized Rayleigh numbers: $1 < r < 1.2$, because of the limitation of present computer power (see [12]).

6 Secondary Bifurcations

In order to trace bifurcation curves by Newton method, we change the parameter:

$$u = u(\mathcal{R}_a), \text{ such that } \mathcal{F}(u, \mathcal{R}_a) = 0,$$
$$u_{n+1} = u_n - \mathcal{F}_u(u_n, \mathcal{R}_a)^{-1}\mathcal{F}(u_n, \mathcal{R}_a), \quad n = 0, 1, 2, \cdots,$$

where u_0 is chosen appropriately. To determine the secondary bifurcation points or the intersection points on the bifurcation curves, we are required to find $u_0, \mathcal{R}_0, \Phi$, such that

$$\mathcal{F}(u_0, \mathcal{R}_0) = 0, \quad \mathcal{F}_u(u_0, \mathcal{R}_0)\Phi = 0.$$

There are difficulties in determining those points, because we use Newton method as above to obtain solutions on bifurcation curves. At the bifurcation point the linearized system has zero eigenvalue, but Newton method needs the inversion of the linearized system for its iteration, which can not be applied at the bifurcation point. However, there are cases that the solution before the bifurcation point belongs to a subspace different from the new solution bifurcating from the bifurcation point. In these cases, we can use these subspaces and Bordering algorism at the bifurcation point, and Newton method for the extended system. Thus we can do numerical computations and computer assisted proof for them.

6.1 The secondary stationary bifurcation point

If

$$u = u(\mathcal{R}_a) \in U_0 \subset\subset U, \text{ such that } \mathcal{F}(u, \mathcal{R}_a) = 0,$$

and

$$\Phi \in U, \text{ such that } \mathcal{F}(u_0, \mathcal{R}_0) = 0, \ \mathcal{F}_u(u_0, \mathcal{R}_0)\Phi = 0,$$

we can take $u, \delta u \in U_0$, $\Phi, \delta\Phi \in U$ and $\mathcal{R}_a, \delta\mathcal{R} \in \mathbb{R}$, such that

$$\begin{pmatrix} \mathcal{F}_u(u, \mathcal{R}_a) & 0 & \mathcal{F}_{\mathcal{R}_a}(u, \mathcal{R}_a) \\ \mathcal{F}_{uu}(u, \mathcal{R}_a)\Phi & \mathcal{F}_u(u, \mathcal{R}_a) & \mathcal{F}_{u\mathcal{R}_a}(u, \mathcal{R}_a)\Phi \\ 0 & 2\Phi^t & 0 \end{pmatrix} \begin{pmatrix} \delta u \\ \delta\Phi \\ \delta\mathcal{R} \end{pmatrix} = \begin{pmatrix} \mathcal{F} \\ \mathcal{F}_u\Phi \\ \|\Phi\|^2 - 1 \end{pmatrix}.$$

Example 6.1 (see [15]) The secondary bifurcation from the mode $(l, n) = (4, 1)$ for $\mathcal{P}_r = 10$, $N = 24$:

$$\mathcal{R}_a = 32.04265 \cdots \times \pi^4, \quad r = \frac{\mathcal{R}_a}{\mathcal{R}_c} = 4.74706 \cdots.$$

The third bifurcation from the mode $(l, n) = (4, 1)$ for $\mathcal{P}_r = 10$, $N = 24$:

$$\mathcal{R}_a = 85.00512 \cdots \times \pi^4, \quad r = \frac{\mathcal{R}_a}{\mathcal{R}_c} = 12.59335 \cdots.$$

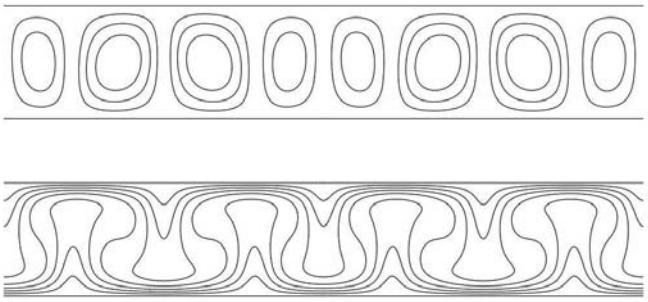

Figure 12 A bifurcated solution from the roll-type solution of mode $(4,1)$ for $\mathcal{R}_a = 13 \times \mathcal{R}_c$

6.2 The secondary Hopf bifurcation point

$$\mathcal{F}(u_0, \mathcal{R}_0) = 0, \quad \mathcal{F}_u(u_0, \mathcal{R}_0)\Phi = \lambda\Phi,$$
$$\lambda = \mathrm{i}\omega, \quad \omega \in \mathbb{R},$$
$$\Phi = \Phi_1 + \mathrm{i}\Phi_2, \quad \Phi_1 \text{ and } \Phi_2 \text{ are real valued},$$
$$\mathcal{F}(u_0, \mathcal{R}_0) = 0, \quad \mathcal{F}_u(u_0, \mathcal{R}_0)\Phi_1 = -\omega\Phi_2, \quad \mathcal{F}_u(u_0, \mathcal{R}_0)\Phi_2 = \omega\Phi_1.$$

Example 6.2 The Hopf bifurcation from the mode $(l, n) = (2, 1)$ for $\mathcal{P}_r = 10$, $N = 24$:

$$\mathcal{R}_a = 277.36398\cdots \times \pi^4, \quad r = 41.09096\cdots, \quad \lambda = \mathrm{i} \times 40.72434\cdots.$$

The Hopf bifurcation from the mode $(l, n) = (2, 1)$ with $\mathcal{P}_r = 10$, $N = 32$:

$$\mathcal{R}_a = 277.36479\cdots \times \pi^4, \quad r = 41.09108\cdots, \quad \lambda = \mathrm{i} \times 40.72440\cdots.$$

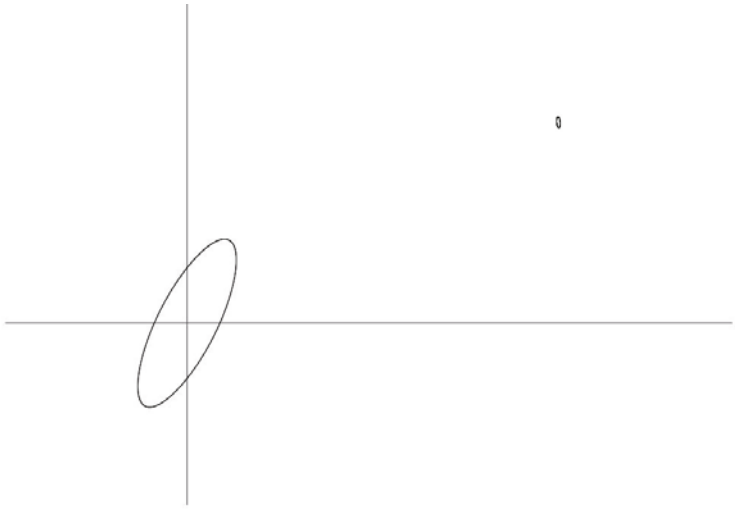

Figure 13 Periodic roll-type solution of mode $(2,1)$ $(4,1)$ for $\mathcal{R}_a = 50 \times \mathcal{R}_c$

This bifurcated time periodic solution can be obtained by the numerical computations of time evolution of the system after time discretization. It suggests its stability contrary

to the bifurcation of periodic solutions of Lorenz model. Figure 13 shows the projection of $(\psi_{2,1}(t), \theta_{2,1}(t))$ and $(\psi_{4,1}(t), \theta_{4,1}(t))$ on the ψ-θ plane.

7 The Bénard-Marangoni Heat Convection where the Upper Boundary is a Free Surface

We refer to [9] for computations of the eigenvalues and eigenfunctions of Bénard-Marangoni problem, which suggests the possibility of both the stationary bifurcation and the Hopf bifurcation from the equilibrium state under the different gravity. These eigenvalues and eigenfunctions can be verified by a computer assisted proof. We proved the existence of both bifurcations for the system of Bénard-Marangoni heat convection in [17, 18].

References

[1] Bénard, H., Les tourbillons cellulaires dans une nappe liquide, *Rev. Gén. Sci. Pure Appl.*, **11**, 1900, 1261–1271, 1309–1328.

[2] Boussinesq, J., Théorie Analytique de la Chaleur, Vol. 2, Gauthier-Villars, Paris, 1903.

[3] Busse, F. H., Non-linear properties of thermal convection, *Rep. Prog. Phys.*, **41**, 1978, 1929–1967.

[4] Crandall, M. G. and Rabinowitz, P. H., Bifurcation, perturbation of simple eigenvalues, and linearized stability, *Arch. Rational Mech. Anal.*, **52**, 1973, 161–180.

[5] Crandall, M. G. and Rabinowitz, P. H., The Hopf bifurcation theorem in infinite dimensions, *Arch. Rational Mech. Anal.*, **67**, 1977, 53–72.

[6] Fujimura, K. and Yamada, S., The 1 : 2 spatial resonance on a hexagonal lattice in two-layered Rayleigh-Bénard problems, *Proc. R. Soc. A*, **464**, 2008, 133–153.

[7] Golubitsky, M., Swift, J. W. and Knobloch, E., Symmetries and pattern selection in Rayleigh-Bénard convection, *Phys. D*, **10**, 1984, 249–276.

[8] Henry, D., Geometric Theory of Semilinear Parabolic Equations, Springer-Verlag, New York, 1981.

[9] Iohara, T., Nishida, T., Teramoto, Y., et al, Bénard-Marangoni convection with a deformable surface, *RIMS Kokyuroku*, **974**, 1996, 30–42.

[10] Joseph, D. D., On the stability of the Boussinesq equations, *Arch. Rational Mech. Anal.*, **20**, 1965, 59–71.

[11] Kawanago, T., Computer assisted proof to symmetry-breaking bifurcation phenomena in nonlinear vibration, *Japan J. Indust. Appl. Math.*, **21**, 2004, 75–108.

[12] Kim, M., Nakao, M. T., Watanabe, Y., et al, A numerical verification method of bifurcating solutions for 3-dimensional Rayleigh-Bénard problems, *Numer. Math.*, **111**, 2008, 389–406.

[13] Kirchgässner, K. and Kielhöfer, H., Stability and bifurcation in fluid dynamics, *Rocky Mountain J. Math.*, **3**, 1973, 275–318.

[14] Lorenz, E. N., Deterministic nonperiodic flow, *J. Atmos. Sci.*, **20**, 1963, 130–141.

[15] Nakao, M. T., Watanabe, Y., Yamamoto, N., et al, A numerical verification of bifurcation points for nonlinear heat convection problems, Proceedings of the Second International Conference on From Scientific Computing to Computational Engineering, Athen, July 5–8, 2006.

[16] Nishida, T., Ikeda, T. and Yoshihara, H., Pattern formation of heat convection problems, Mathematical Modeling and Numerical Simulation in Continuum Mechanics, I. Babuska, P. G. Ciarlet and T. Miyoshi (eds.), Springer-Verlag, New York, 2001, 209–218.

[17] Nishida, T. and Teramoto, Y., On a linearized system arising in the study of Bénard-Marangoni convection, Proceedings of the International Conference on Navier-Stokes Equations and their Applications, 2006, 1–20; *RIMS Kokyuroku Bessatsu*, **B1**, 2007, 271–286.

[18] Nishida, T. and Teramoto, Y., Bifurcation theorems for the model system of Bénard-Marangoni convection, *J. Math. Fluid Mech.*, published online, 2007. DOI:10.1007/s00021-007-0263-9

[19] Oberbeck, A., Über die Wärmeleitung der Flüssigkeiten bei der Berücksichtigung der Strömungen infolge von Temperaturdifferenzen, *Ann. Phys. Chem.*, **7**, 1879, 271–292.

[20] Ogawa, T., Hexagonal patterns of Bénard heat convection, *RIMS Kokyuroku*, **1368**, 2004, 144–151.

[21] Rayleigh, L., On convection currents in a horizontal layer of fluid, when the higher temperature is on the under side, *Phil. Mag.*, **32**, 1916, 529–546.

[22] Urabe, M., Galerkin's procedure for nonlinear periodic systems, *Arch. Rational Mech. Anal.*, **20**, 1965, 120–152.

[23] Watanabe, Y., Yamamoto, N., Nakao, M., et al, A numerical verification method for bifurcated solutions of Rayleigh-Bénard problems, *J. Math. Fluid Mech.*, **6**, 2004, 1–20.

[24] Yudovich, V. I., On the onset of convection, *J. Appl. Math. Mech.*, **30**, 1966, 1193–1199.